

Emergence of Supersteps on KH_2PO_4 Crystal Surfaces

T. N. Thomas,^{1,2} T. A. Land,^{2,*} W. H. Casey,^{1,3} and J. J. DeYoreo²

¹Department of Land, Air, and Water Resources, Chemistry Graduate Group, University of California, Davis, California 95616, USA

²Chemistry and Materials Science Directorate, Lawrence Livermore National Laboratory, Livermore, California 94551, USA

³Department of Geology, University of California at Davis, Davis, California 95616, USA

(Received 16 January 2004; published 28 May 2004)

In situ AFM investigation of growth on the {100} face of KH_2PO_4 in the presence of Al(III) and other trivalent metals reveals the emergence of a new type of morphological feature—the superstep. Supersteps, or step bunches consisting of 50–1500 elementary steps, are responsible for growth at all supersaturations and exhibit behavior not predicted by accepted models. The step velocity of the superstep is greater than that of single atomic steps and increases with step height. The steepness of the step riser reaches a limiting value of only 11.8° .

DOI: 10.1103/PhysRevLett.92.216103

PACS numbers: 68.35.-p, 68.37.Ps

Introduction.—Since the advent of the modern theory of crystal growth, the elementary step has been viewed as the central feature of a growing crystal surface [1]. Likewise, growth inhibition by impurities has been analyzed in terms of the pinning of elementary steps due to their interaction with the adsorbates [2]. The realization that these interactions can produce step pileup led to the inclusion of the term “macrostep” into the lexicon of crystal-growth science [3–5]. This step-bunching behavior has also been observed in interferometric investigations of crystal growth from solution [6–9]. However, unlike atomic force microscopy (AFM), interferometric length scales are too large to show the details of step bunching such as step height and terrace width. Traditionally, macrostep formation has been viewed as detrimental to growth, leading to trapping of impurities and slowing growth of the crystal face. Thus, in a wide range of scientific disciplines, impurities—either naturally occurring or intentionally introduced—have been the focus of intense research [3–5, 10, 11]. Recently, Land *et al.* [12] showed that, during regeneration of growth following impurity poisoning, macrosteps can play the central role once attributed to elementary steps. Here we report the discovery of yet a new family of steps that consist of hundreds or thousands of elementary steps. These “supersteps”—also induced by impurity adsorption—travel at speeds far in excess of either elementary steps or macrosteps and exhibit behavior starkly different from that predicted by standard models.

The inhibition of growth by impurities is conventionally described by the Cabrera-Vermilyea (C-V) model [2] in which the normal flow of a train of elementary steps across the growing crystal face is disrupted as the steps are pinned by a field of adsorbed “impurity stoppers.” These stoppers create a so-called “dead zone” in which the step is prevented from advancing because the critical radius of step curvature ($r_c = \alpha\omega/kT\sigma$) is (approximately) greater than the impurity spacing (where α is

the step-edge free energy, ω is the molecular volume, k is Boltzmann’s constant, T is temperature, and σ is supersaturation). If the supersaturation is increased, a critical value, σ^* , is reached at which the critical radius falls below the average impurity spacing and the elementary steps begin to move again. According to the C-V model, the surface then once again consists of a moving train of elementary steps.

Previously, Land *et al.* demonstrated that this classic picture does not account for the observed behavior caused by Fe(III) poisoning of the solution-grown crystal KH_2PO_4 (KDP) [12]. Instead, the recovery of the KDP surface occurred through the movement of macrosteps, which were mobile even when elementary steps remain pinned. This led to a slow increase in growth rate below σ^* , even for supersaturations in the region $\sigma_d < \sigma < \sigma^*$. From the width of the slow-growth region, a characteristic adsorption time for Fe impurities onto the surface of KDP was derived by considering a model for macrostep propagation through a field of immobile elementary steps [12]. Surprisingly, the addition of Al(III) to KDP produces entirely different behavior, not predicted by either model.

Methods.—The details of the experimental procedure are discussed in depth elsewhere [12, 13]. Typical Al(III) and Fe(III) concentrations were 7.5 and 15 μmol Al(III) or Fe(III) per mole KDP. Solutions were allowed to equilibrate at 80 °C for several hours before experimentation. Dopant concentrations were confirmed via elemental analysis.

Results and discussion.—Figure 1 shows a plot of step speed, v , vs σ for the growth of KDP in the presence of Al(III) at a concentration of 15 μmol per mole of KDP (3.0 ppm by weight), along with the observed surface morphology at four separate points along the curve. Also shown in Fig. 1 is a typical curve for the Fe(III)-KDP system at the same dopant concentration. For the Al-bearing system, because of step pinning, the step

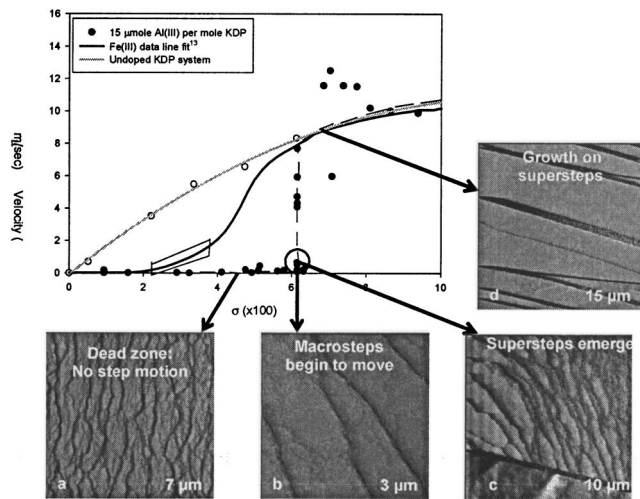


FIG. 1. Step velocity vs percent supersaturation (σ) for pure solution (grey line) and solution containing $15 \mu\text{mol Al(III)}$ per mole KDP. The solid black line is a calculated line fit to the velocity curve for an equivalently doped Fe(III) system [14]. (a) For all supersaturations below σ^* (circled in black), the elementary and macrosteps are pinned. (b) Macrosteps begin to move at σ^* , leaving the elementary steps immobile on the surface. (c) Before the macrosteps can fully recover growth, supersteps appear and quickly overcome the slow moving macrosteps. (d) For $\sigma > \sigma^*$, supersteps dominate the growth surface. The boxed region on the Fe(III) line marks the slow growth region where $\sigma_d < \sigma < \sigma^*$.

velocity of the $\{100\}$ face is approximately zero up to σ^* and, unlike the case of Fe(III), no slow-growth region is observed [Fig. 1(a)] below σ^* . Both the elementary and macrosteps characteristic of KDP growth are present, but are immobile. Moreover, as the supersaturation is increased, growth does not recover on elementary steps at any Al(III) concentration. Instead, elementary steps bunch together to form macrosteps consisting of 2 to 12 elementary steps [15]. As in the case of Fe(III), these macrosteps are the first class of steps to begin advancing [Fig. 1(b)] as the surface recovers from the dead zone. At σ^* , they begin to move while the elementary steps remain pinned. More significantly, precisely at σ^* , just as the macrosteps become mobile and while the elementary steps are still pinned, a new class of step bunches we call supersteps appears [Fig. 1(c)]. They move across the surface through the field of macrosteps and elementary steps, apparently unimpeded by the adsorbed impurities.

The supersteps consist of hundreds to thousands of elementary steps that are tightly spaced and move as a single advancing step. They can form anywhere on the $\{100\}$ face of KDP, including near the top of dislocation growth hillocks that provide the sources of steps on this surface (Fig. 2). The supersteps can be up to 500 nm tall and quickly replace all other morphological features as they move across the surface. Close to σ^* , the motion of supersteps across the face is erratic: They appear at ir-

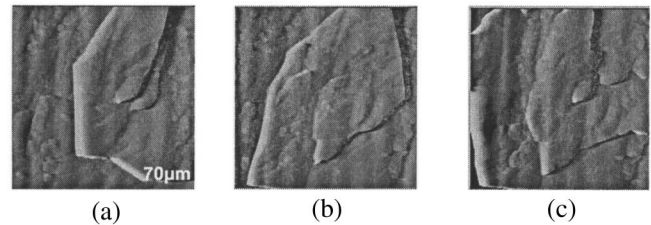


FIG. 2. Formation of supersteps at the apex of a dislocation growth hillock. (a)–(c) The motion of a superstep about the dislocation over three subsequent scans. These images were taken in a system highly doped with Fe(III) ($45 \mu\text{mol}$ per mole KDP or 15 ppm by weight).

regular intervals and are inconsistent in height. The supersteps rapidly increase in velocity over a small range of σ (see graph in Fig. 1). Above the dead zone, the supersteps achieve the velocities of elementary and macrosteps measured in pure solutions at the same supersaturation. We have observed this behavior for all concentrations of Al(III) investigated, as well as for high concentrations of Fe(III) [$> 45 \mu\text{mol Fe(III)}$ per mole KDP]. As supersaturation is varied about σ^* , the supersteps form and disintegrate (Fig. 3).

A brief transition region occurs during the initial recovery from the dead zone in which elementary, macrosteps, and supersteps are expressed simultaneously on the surface. During this transition period, although the supersteps advance quickly, elementary steps remain pinned

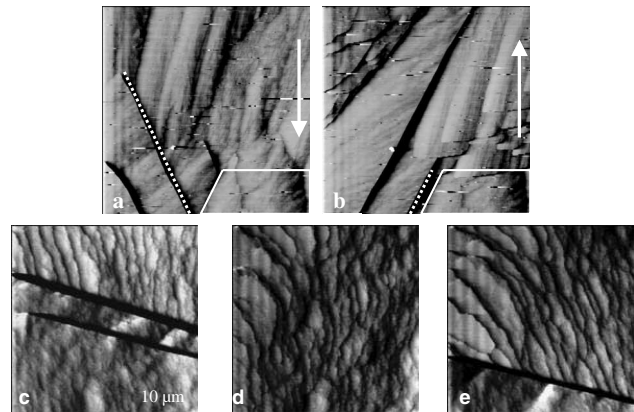


FIG. 3. Formation and disintegration of supersteps. As supersaturation varies about σ^* , supersteps form and disintegrate across the entire $\{100\}$ face ($20 \mu\text{m}$ scan). (a) The formation of a superstep (highlighted in dotted line) captured in a downward scan. (b) The subsequent upward scan shows the same superstep, disintegrating into macrosteps that remain motionless on the surface. The macrosteps and elementary steps (outlined in solid lines) are not passed over by a superstep during the collection of the two images and thus remain unchanged. (c)–(e) Motion of three separate supersteps across the surface during the resurrection from the dead zone. Note: The macrosteps in (d) are immobile.

and small macrostep bunches become slightly mobile. All macrosteps and elementary steps visible on the surface are quickly incorporated into the advancing superstep, which, in essence, creates a “fresh” surface as it advances [see Figs. 1(c) and 3]. This new surface then begins to grow again via the creation and movement of macrosteps, which are quickly incorporated into an advancing superstep. This process continues during the brief transition region that spans only $\sigma = +0.01$. Beyond the transition region, supersteps alone dominate the growth surface for the remainder of the supersaturation range investigated here.

The recovery of the growth surface from the dead zone on such large step bunches is surprising enough. In addition, we find that the supersteps exhibit behavior unexpected for step bunches of any size. First and most significantly, the step velocity is directly proportional to the number of elementary steps in a superstep [Fig. 4(a)]. This behavior contrasts directly with classic theories of macrostep propagation in which taller bunches of steps are predicted to move more slowly due to mass-transport limitations. However, this height dependence of velocity is apparently true only for the narrow supersaturation range in which recovery from the dead zone takes place [$\sigma = 6\%–7\%$ for the $15 \mu\text{mol}$ per mole Al(III) concentration]. At supersaturations where the step velocities are similar to those in an undoped system, all superstep and macrostep velocities are equal to within the error of our measurements, regardless of height.

Our results also show that, although the step-riser angle increases with step height, this increase persists only to step-bunch heights of roughly 300 nm (800 elementary steps). Supersteps above 300 nm tall consistently have a step-riser angle of approximately 11.8° [Fig. 4(b)]. This limiting angle apparently lends stability to the superstep. We consider three possible explanations for its appearance. (1) The angle is that of a thermodynamically stable microfacet, so that growth no longer occurs at step edges of the $\{100\}$ face but rather on step edges of this new face. If growth on this microfacet were unaffected by Al(III) impurities—as on the $\{101\}$ face—then the step speed should be considerably larger. A quantitative analysis of this scenario, however, quickly shows that it is impossible. The step speeds required along a facet that lies at 11.8° off of $\{100\}$ to result in the observed superstep velocity are many orders of magnitude too large to be realistic.

(2) Entropic repulsion between steps results in the observed riser angle. Even at equilibrium, step edges are not static but wander forward and backward to maximize entropy, but are limited by the step stiffness (the variation in step-edge free energy with step orientation). Consequently, two steps cannot come arbitrarily close to one another without interfering with each other’s ability to wander. The result is an effective force referred to as entropic repulsion. A superstep riser angle of 11.8°

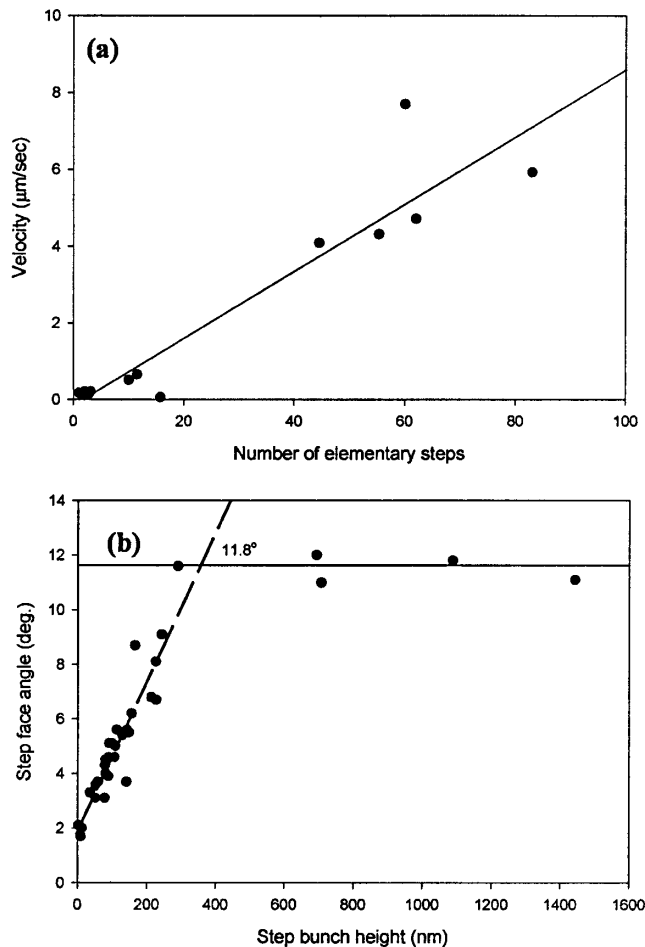


FIG. 4. (a) During the resurrection from the dead zone, the velocity of a step bunch is directly proportional to the number of elementary steps [$15 \mu\text{mol}$ Al(III) per mole KDP, $\sigma^* = 0.063$]. (b) The riser angle of a step bunch rises linearly with step height until the height is approximately 300 nm. Beyond this height the riser angle reaches a limiting value of 11.8° (taken from *ex situ* analysis of crystals).

corresponds to an 18 \AA terrace width between elementary steps, or about five lattice spacings. On the $\{100\}$ face of KDP, the amplitude of step wandering averages about ± 10 lattice sites, which argues for consideration of entropic repulsion as the source of the limiting riser angle [14].

(3) The observed riser angle results from a consideration of terrace lifetimes and impurity adsorption rates. As steps bunch together, the terrace lifetime decreases, eventually falling below the characteristic adsorption time for impurities. Although there are a number of theories for impurity induced step bunching, it is impurity adsorption that drives the instability leading to the formation of macrosteps. If impurity adsorption is prevented, the driving force for bunching is removed. Hence, once the terrace lifetime becomes less than the impurity adsorption time, the driving force for bunching should begin to decline.

The terrace width would reach a limiting value and the superstep speed could approach that of steps in the undoped system. In contrast, the elementary and macrosteps should still be susceptible to pinning due to their larger terrace widths, which allow impurities to accumulate. For an 18 Å terrace width between elementary steps in a superstep moving at 9 μm/s, the terrace lifetime is of order 200 μs. Thus, one would conclude that the adsorption time for Al is $\geq 200 \mu\text{s}$. In comparison, Land *et al.* concluded that Fe(III) had an adsorption time on the order of 1–10 s [12], leading to the slow rise from the dead zone ($\sigma_d < \sigma^*$) discussed earlier and illustrated in Fig. 1. In the Al(III) doped system, there is no slow rise out of the dead zone ($\sigma^* = \sigma_d$), which implies a short adsorption time for Al(III) [12] and is consistent with this model for the limiting riser angle. We note, however, that the inferred relative adsorption times of Fe(III) and Al(III) are opposite from what is expected from ligand exchange around simple Fe(III) and Al(III) complexes. This may reflect differences in surface speciation or surface diffusion.

The results presented here further demonstrate the rich behavior of the KDP system. In contrast to classic models of growth, the surface of this crystal expresses three families of steps, each with unique characteristics and acting independently of the others. In particular, in the presence of Al(III) and high concentrations of Fe(III), a previously undiscovered family of steps emerges, which we have called supersteps. This discovery calls for a reevaluation of traditional growth models to account for the presence of these morphological features in order to fully understand the regeneration of a crystal surface from impurity poisoning. While this and the previous paper by Land *et al.* [12] presented rudimentary models, a detailed physical understanding still remains to be established.

We thank Dave Wruck, Tracy Martin, Ana Villacampa, and U.S. DOE Grant No. DE-FG03-02ER15325

(to W.H.C.) for support. This work was performed under the auspices of the U.S. Department of Energy by Lawrence Livermore National Laboratory under Contract No. W-7405-Eng-48 (UCRL-JC-152309).

*Author to whom correspondence should be addressed.

Electronic address: land1@llnl.gov

- [1] F. C. Frank, *Growth and Perfection of Crystals* (Wiley, New York, 1958), p. 411.
- [2] N. Cabrera and D. A. Vermilyea, *Growth and Perfection of Crystals* (Chapman and Hall, London, 1958), Vol. 393.
- [3] A. McPherson, *Crystallization of Biological Macromolecules* (Cold Spring Harbor Laboratory Press, Cold Spring Harbor, New York, 1999).
- [4] A. J. Malkin *et al.*, *Nat. Struct. Biol.* **2**, 956 (1995).
- [5] C. M. Pina, U. Becker, P. Risthaus, D. Bosbach, and A. Putnis, *Nature (London)* **395**, 483 (1998).
- [6] A. A. Chernov and A. I. Malkin, *J. Cryst. Growth* **92**, 432 (1988).
- [7] Yu. G. Kuznetsov, A. A. Chernov, and N. D. Zakharov, *Krystallografiya* **31**, 1201 (1986).
- [8] I. L. Smol'skii, A. I. Malkin, A. A. Chernov, *Krystallografiya* **31**, 769 (1986).
- [9] A. A. Chernov, L. Rashkovich, and A. A. Mkrтчan, *J. Cryst. Growth* **74**, 101 (1986).
- [10] N. P. Zaitseva *et al.*, *J. Cryst. Growth* **180**, 255 (1997).
- [11] H. H. Teng, P. M. Dove, C. A. Orme, and J. J. DeYoreo, *Science* **282**, 724 (1998).
- [12] T. A. Land, T. L. Martin, S. Potapenko, G. T. Palmore, and J. J. DeYoreo, *Nature (London)* **399**, 442 (1999).
- [13] T. N. Thomas, T. A. Land, T. Martin, W. H. Casey, and J. J. DeYoreo, *J. Cryst. Growth* **260**, 566 (2003).
- [14] L. N. Rashkovich and N. V. Kronskey, *J. Cryst. Growth* **182**, 434 (1997).
- [15] J. J. DeYoreo, A. K. Burnham, and P. K. Whitman, *Int. Mater. Rev.* **47**, 113 (2002).